Photocycloreversions within single polymer chains†

Modan Liu,[a] Wolfgang Wenzel *[a] and Hendrik Frisch *[b,c]

Reversible photocycloadditions hold great potential for the development of remote-controlled chemical networks: the bond forming cycloaddition can be initiated with one wavelength, while the formed cycloadduct can be reversed upon irradiation with a shorter wavelength. Herein, we investigate photocycloreversions within the confined environment of single polymer chains and reveal that the orthogonal addressability of cycloaddition and cycloreversion is drastically limited within the polymer coil: both, shorter and longer wavelengths (λ = 330 and 430 nm) induce effective intra–macromolecular crosslinking of single polymer chains into single chain nanoparticles (SCNPs). To elucidate the experimentally observed behaviour, we developed a comprehensive model based on coarse-grained molecular dynamics (MD) simulations, which allows simulation of the number of crosslinking points along with the morphology of the polymer coil under different irradiation wavelengths. The combination of experimental results and simulation revealed that irradiation at a shorter wavelength (λ = 330 nm) gives rise to a photostationary state where photocyclo-addition and -reversion are occurring concomitantly. Under these conditions, covalent bonds are constantly formed and broken, allowing a dynamic rearrangement of the intra-macromolecular crosslinks of the SCNP, yet no decrosslinking into the linear precursor polymer. The developed SCNP system may serve as a blueprint for understanding the effect the confined environment has on photostationary states within polymer networks.

Introduction

Motivated by the plethora of functions that nature enables in macromolecules, around a decade ago polymer chemists began to investigate the intramolecular crosslinking of synthetic polymers into single chain nanoparticles (SCNPs) to mimic the complexity of natural macromolecules.[1–3] Among other applications, the unmatched reaction control of enzymes has inspired the development of catalytically active SCNPs as synthetic nanoreactors.[4,5] Unlike natural systems, which are limited to the pool of amino acids, synthetic systems are merely limited by the polymer chemist's creativity.[6–8] As a consequence, limitations of enzymatic catalysts, including scope of reactions, solvents and temperature, could be overcome through the design of synthetic single chain nanoreactors.[9–17] Establishing remote control over the morphology of catalytically active SCNPs, through a folding and unfolding of synthetic polymer chains, holds a potential to regulate catalytic activity on unprecedented levels.[4] Until today, reversible folding and unfolding and SCNPs requires the addition of solvents,[18] competing guest-molecules,[19] photoinitiators,[20] oxidation agents,[21] mechanical forces[22,23] or elevated temperatures.[25,26] In contrast to such drastic changes of the chemical and physical environment, which are likely to interfere with the catalytic activity of the SCNP, light gated reactions are in most cases orthogonal to the catalysed reaction and can also be executed under spatiotemporal control.[27–29]

Photoreversible cycloaddition reactions are a highly promising class of reactions to form and break crosslinking points with light.[30] Since photocycloaddition reactions decrease the size of the conjugated systems of the involved chromophore, the absorbance of the photoproduct is hypsochromically shifted and irradiation at shorter wavelengths induces the bond breaking cycloreversion reaction. However, despite these photoreversible reactions, a complete light gated folding and unfolding of SCNPs has not been achieved. When the [2 + 2] photocycloaddition of coumarin[31] or the [4 + 4] photocycloaddition of anthracene[32] was seized to fold SCNPs, subsequent irradiation with shorter UV light (λ = 254 nm) has thus far not

[a]*Institute of Nanotechnology (INT), Hermann von Helmholtz Platz 1, 76344 Eggenstein Leopoldshafen, Karlsruhe Institute of Technology (KIT), Germany. E mail: wolfgang.wenzel@kit.edu*

[b]*School of Chemistry and Physics, Queensland University of Technology (QUT), 2 George Street, Brisbane, QLD 4000, Australia. E mail: H.Frisch@qut.edu.au*

[c]*Centre for Materials Science, Queensland University of Technology (QUT), 2 George Street, Brisbane, QLD 4000, Australia*

†Electronic supplementary information (ESI) available: Additional experiments, experimental details, detailed description of the simulations and a movie of the simulated photoreactive polymer in different photonic fields. See DOI: 10.1039/d0py01062f

achieved a full unfolding of the SCNP to recover the parent polymer. Herein, we explore photocycloreversion reactions within single polymer chains and develop a comprehensive model to reveal the effect of irradiation wavelength on the number of crosslinking points and size of the SCNP. A particularly versatile photoreactive molecule to study photocycloreversions is styrylpyrene, as it allows for mild irradiation wavelengths to induce the cycloaddition (λ > 400 nm) and cycloreversion (330 nm, Fig. 1a and b).[33–35] Due to these mild irradiation wavelengths, even long irradiation times at the cycloreversion wavelengths have a significantly lower probability of photodamage to the polymer backbone or the photoreactive unit, compared to harsh 254 nm light required for anthracene, coumarin or stilbene moieties.[30] Attached to the termini of polymers, styrylpyrene has been successfully applied as a remote controlled biding site that allows to ligate two polymer chains under visible light irradiation (λ = 430 nm) and cleave them subsequently with UV light (λ = 330 nm).[27,34–36] Key to this wavelength selectivity is that styrylpyrene absorbs light in the visible range, while the cycloadduct absorbs exclusively below 400 nm. Visible light thus initiates exclusively the photocycloaddition. In contrast, both styrylpyrene and its photocycloadduct absorb UV light, whereas the intramolecular cycloreversion is strongly favoured over the bimolecular cycloaddition that competes with radiative and non-radiative deexcitation pathways in these examples.[27,34–36] Based on a copolymer of methyl methacrylate (MMA) and a styrylpyrene containing monomer (M1), we have recently investigated the styrylpyrene induced single chain folding into SCNPs.[24] We observed that both the quantum yield and wavelength dependence of the cycloaddition reaction were affected by the macromolecular confinement.

Results and discussion

To investigate the cycloreversion reaction within single polymer chains, **SCNP1**, which was obtained through irradiation of **P1** (Table 1)[24] with 6.2×10^{-5} mol photons at λ = 430 nm, was subsequently irradiated with λ = 330 nm light (0.55 mg mL^{-1} **SCNP1** in THF). To address the cycloaddition or cycloreversion reaction as selectively as possible, monochromatic laser light was used for all irradiation experiments (ESI chapter 3.1†). As previously reported, the reaction was monitored by UV/vis spectroscopy following the absorption maximum of styrylpyrene at λ = 383 nm (Fig. 2b).[24] It can be observed that the absorbance initially increases, as expected for the cycloreversion reaction due to a decrease of cyclobutane species and an increase of styrylpyrene (Fig. 2c).[37] After the

Table 1 Physicochemical data of and monomer ratio (m/n) of photo reactive P1[24] and P1′

	M_n/g mol^{-1} (SEC, PMMA cal.)	$Đ$ (SEC)	*Styrylpyrene content* (^{1}H NMR)	*m/n* (^{1}H NMR)
P1	13 600	1.22	28%	17/44
P1′	19 300	1.26	30%	25/58

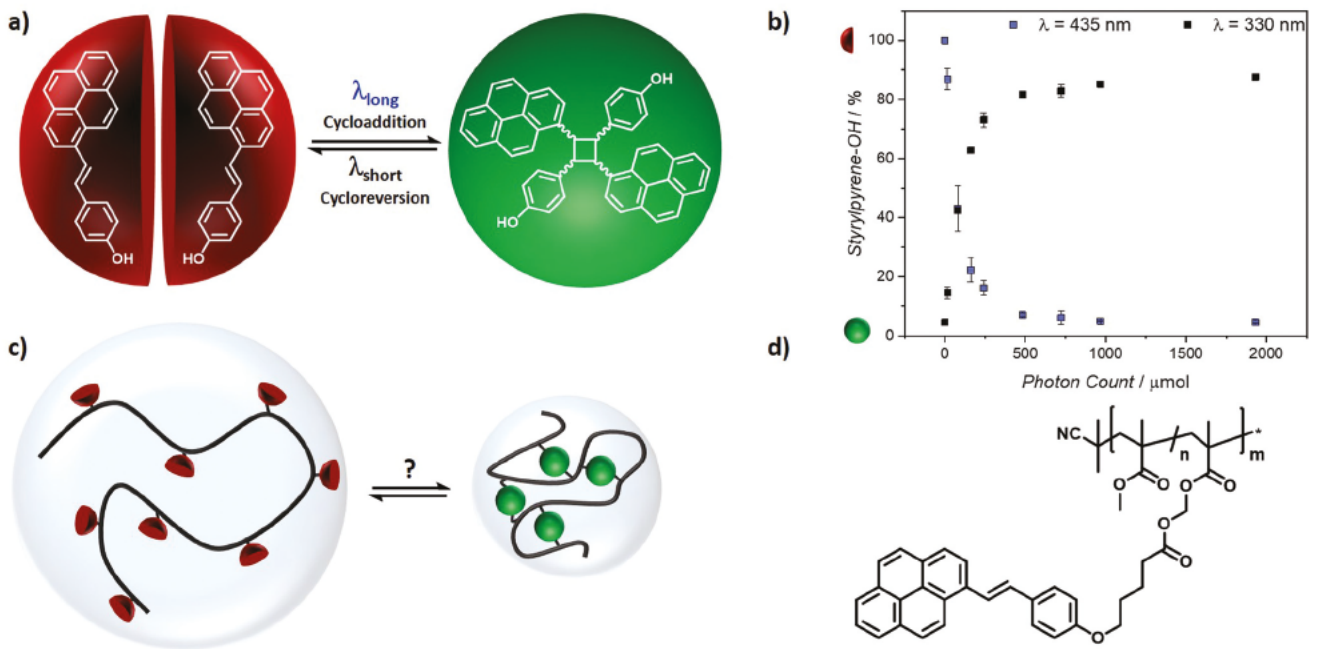

Fig. 1 (a) Chemical structure and schematic representation of the photoreversible [2 + 2] cycloaddition of styrylpyrene. (b) Photocycloaddition and photocycloreversion of hydroxy styrylpyrene in dependence on the number of incident photons as reproduced from ref. 35. (c) Within the confined environments of single polymer chains, the kinetics of the reaction are drastically altered, affecting a reversible folding and unfolding of the polymer into a single chain nanoparticle. (d) Chemical structure of the herein investigated styrylpyrene containing polymers P1 and P1′.

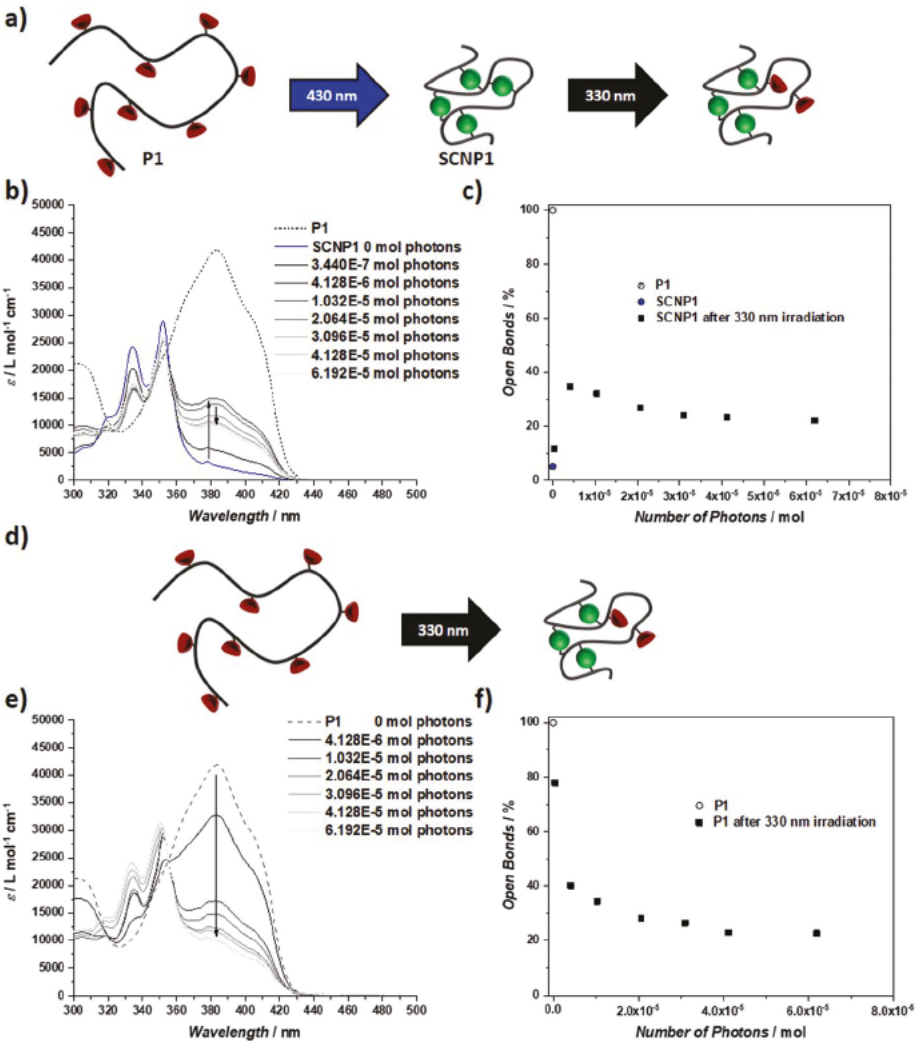

Fig. 2 (a) Schematic depiction of the single chain folding of P1 induced by excusive photocycloaddition at λ = 430 nm yielding SCNP1, followed by subsequent irradiation at λ = 330 nm inducing a partial cleavage of crosslinks, which is limited by a photostationary state of competing cycloaddition and cycloreversion. (b) UV/vis spectra of SCNP1 after irradiation with UV light (λ = 330 nm). (c) Open photoreactive crosslinks within SCNP after irradiation with UV light (λ = 330 nm) (d) schematic representation of the UV light induced SCNP folding of P1, yielding a partially folded SCNP. (e) UV/vis spectra of P1 after irradiation with UV light (λ = 330 nm). (f) Open photoreactive crosslinks within P1 after irradiation with UV light (λ = 330 nm).

initial increase yielding close to 35% of open bonds, the number of crosslinks decreases again, reaching a plateau close to 22% of open crosslinking points. These findings are in stark contrast to the behaviour observed for the cycloreversion of hydroxy-styrylpyrene, where close to quantitative cycloreversions can be achieved upon irradiation at λ = 330 nm (compare Fig. 1b).[35] The selective addressability of either cycloaddition or cycloreversion observed in solution is consequently lost within the strongly confined environment of polymer chains. Photodimers that are cleaved in free solution under irradiation at λ = 330 nm can diffuse apart after cycloreversion, however, the tethering of the photoreactive molecules to the polymer backbone holds the photoreactive molecules in close proximity. As a consequence, the strongly diffusion dependent photocycloaddition reaction, which competes with radiative and non-radiative deexcitation processes, becomes kinetically more favoured and the predominant reaction over the monomolecular cycloreversion – even in the UV regime. To fold and unfold SCNPs, based on the photoreversible cycloaddition of styrylpyrene only by irradiation with either UV or visible light, is thus not feasible.

To determine whether the observed photostationary state is influenced by the initial compaction into an SCNP, the linear parent polymer **P1** was irradiated with UV light at λ = 330 nm (Fig. 2e). Upon irradiation, the number of crosslinks increases as indicated by the decreasing absorption of styrylpyrene. The plateau reached at around 23%, which is comparable to the number of crosslinks observed for UV light irradiation of the crosslinked **SCNP1** (Fig. 2f). UV light irradiation consequently induces cycloaddition and cycloreversion concomitantly yield-

ing a dynamic covalent SCNP, in which the majority of photoreactive bonds is in a closed state. It is thus possible to induce the intramolecular crosslinking of **P1** with both visible and UV light, yet yielding different crosslinking degrees of the resulting SCNPs.

To investigate the effect of polymer chain lengths, **P1′** was synthesized containing a comparable percentage content of photoreactive units, yet a close to 40% higher molecular weight (M_n = 19 300 g mol^{-1}, $Đ$ = 1.26, Table 1). Upon irradiation with visible light (λ = 430 nm), a decrease of styrylpyrene absorption was observed, reaching a plateau at 96%, slightly below the crosslinking degree of **P1** (Fig. S1 and S2†). To combine the crosslinking degree with the compaction of the macromolecules, size exclusion chromatography (SEC) was employed. After irradiation with 1.9 × 10^{-5} mol photons (λ = 430 nm), the elution maximum increases from 21.8 to 22.2 mL as expected for the more compact conformation of a crosslinked SCNP (Fig. 3a, blue line).

If the resulting **SCNP1′** is subsequently irradiated with UV light, the number of crosslinks decreases initially, as observed for **SCNP1**, increases subsequently and reaches a plateau at 25% (Fig. S3 and S4†). UV light irradiation with 1.0 × 10^{-5} mol photons decreases the elution volume in the SEC from 22.2 to 22.0 mL resulting from a partial unfolding of **SCNP1′** (Fig. 3b). Under initial irradiation with UV light **P1′**, reaches a comparable photostationary state of a crosslinking degree of 24% (Fig. S5 and S6†) and an elution volume of 22.0 mL after irradiation with 1.0 × 10^{-5} mol photons (Fig. 3b). Remarkably, under the same concentrations (0.5 mg mL^{-1}) as applied for visible light irradiation, the UV light induced folding results in a more pronounced shoulder at higher molecular weights indicating intermolecular chain coupling. The higher propensity of interchain coupling under UV light irradiation likely results from the dynamic nature of the covalent bonds under UV irradiation. Visible light exclusively excites styrylpyrene, which decreases the number of available crosslinking sites rapidly and with a higher quantum yield for the intramolecular over the intermolecular reaction.[24] After exposure to 1.0 × 10^{-5} mol photons, the concentration of available binding sites has been irreversibly decreased by almost 90% and the remaining binding sites might be of limited sterical accessibility. Under UV light irradiation, however, both cycloaddition and -reversion take place concomitantly. The resulting crosslinks are frequently formed and broken, which maintains a higher number of available crosslinks throughout the entire experiment. Interchain coupling thus becomes more favourable under UV light irradiation, whereas the dynamic separation of two crosslinked polymer chains is inhibited by the high multivalence of two crosslinked chains. To control the folding of SCNPs reversibly within the borders of the photostationary state by triggering of the cycloreversion reaction, more dilute reaction conditions are required compared to a purely cycloaddition induced SCNP folding.

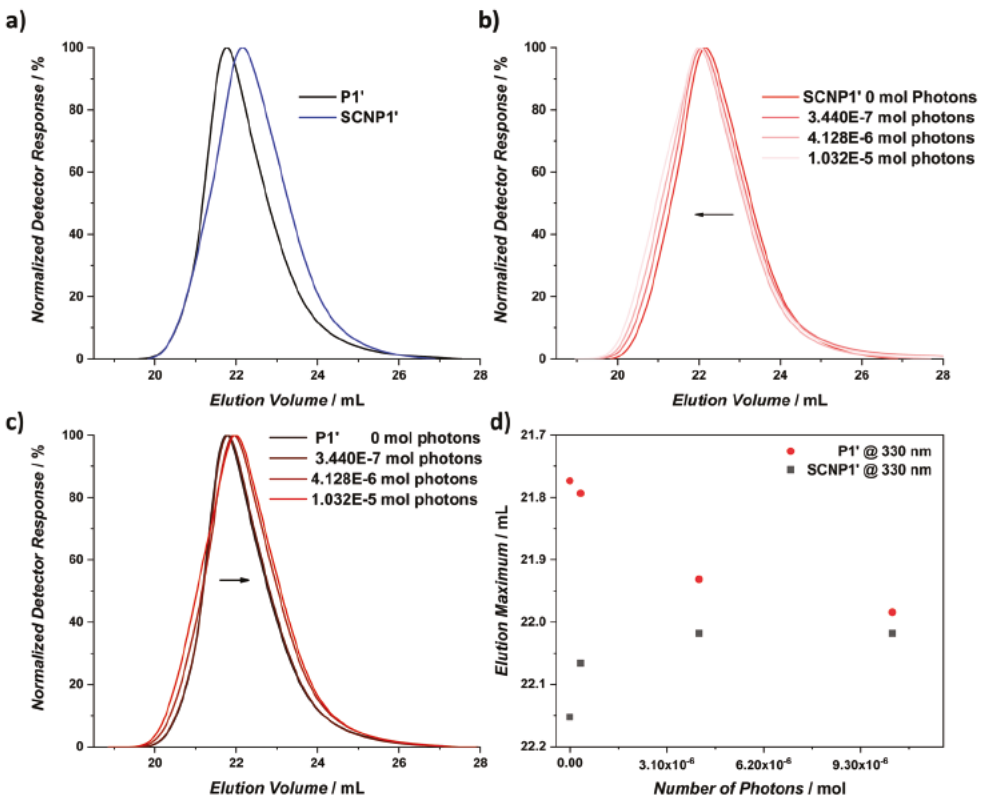

Fig. 3 (a) SEC trace of P1′ and of the resulting SCNP1′ after irradiation with blue light (λ = 430 nm). (b) SCNP1′ after irradiation with UV light (λ = 330 nm). (c) P1′ after irradiation with UV light (λ = 330 nm). (d) Elution maximum of the polymers obtained from the SEC traces displayed in b and c.

To gain a deeper understanding of the dynamic bond formation and fission under UV light irradiation, and its effect on the folded SCNPs, we performed molecular dynamics (MD) simulations with dissipative particle dynamics (DPD),[38,39] which is a widely used coarse-grained (CG) model for polymer simulations. A proper description of diffusion dynamics was achieved by coupling DPD with a segmental repulsive potential (SRP) corrected finitely extensible nonlinear elastic (FENE) bonding model; the model is described in detail in the ESI.†

The coarse-grained DPD model obeys the fluctuation-dissipation relation, which introduces an inherent timescale that can be used to interpret the diffusion process. The model used for the polymer and its intra-macromolecular bond formation and fission is sketched in Fig. 4. To model diffusion and bond recombination on the styrylpyrene group, we divide the monomers and THF solvent into 5 DPD types of units as described in the ESI.† The DPD characteristic length, mass, and energy are then chosen as L_{DPD} = 1.0 nm, m_{DPD} = 100 Da and ε_{DPD} = k_BT = 4.1416^{-21}J at 300 K. MD simulation timestep $\Delta t$is chosen to be 0.01τ_{DPD}, where the intrinsic time scale of DPD τ_{DPD} ¼ $L_{DPD}\sqrt{m_{DPD}/\varepsilon_{DPD}}$ ¼ 7 ps.

Dynamic bond formation and fission in MD is modelled by a local stochastic process. A bond can be formed with finite probability when a pair of non-crosslinked photoreactive sites get within the threshold distance of 1.5L_{DPD}. For crosslinked units there is a certain probability that the covalent bond is broken (see ESI†). Reaction processes are attempted at a rate that is fixed to reproduce the timescale difference between diffusion and chemical reaction. Both values are fitted to experimental measurements of **P1**, detailed in the ESI chapter 5.† An ensemble of 500 distinct initial conformations are generated for **P1** and **P1′** with 61 and 83 monomer units, respectively, in accordance to the experimental size distribution of the polymers. Photoreactive monomer units are uniformly distributed among the sites of the polymer chain following Gaussian distribution centred around 28% for **P1** and 30% for **P1′**.

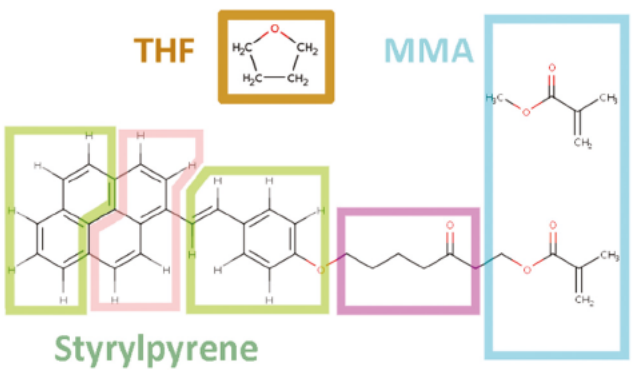

Fig. 4 Coarse graining scheme for polymer THF system for DPD simu lations. MMA and M1 monomers share a common base unit, while 3 extra units are introduced to represent M1 monomers based on chemi cal properties as group molecular weight and shape. A 3 component styrylpyrene complex is bound by strong FENE bonds to reflect shape, whilst preserving a crosslinking candidate site, shown in pink color, in MD simulation visualization in the ESI chapter 5† it can be shown between 3 component styrylpyrene complexes the photocycloaddition reaction yields both head to head and head to tail dimer conformations.[35]

A movie that illustrates the dynamic nature of the process an individual trajectory that shows how **P1** folds into **SCNP1** when subjected to 330 nm light and subsequently unfolds when subjected to 430 nm, is included in the as supplementary material (movie S1†). Along the MD trajectory the time series for the ratio of open bonds and radius of gyration of both the simulated polymer, and the crosslinked SCNP are recorded. Statistical averages, obtained from the MD simulations, are shown in Fig. 5. Consistent with observations from experiments, the polymer coil constantly changes morphology. However, when irreversible bond formation starts to constrain morphology, dimerization is synchronous with the process of compaction from **P1** to **SCNP1** (blue trace, Fig. 5). When the compact conformation is subjected to 330 nm light, dynamic bond formation and fission reorganize the bonding in the crosslinking sites (red trace, Fig. 5). Of particular interest is the observation that the release from a constrained conformation leads to a more unfolded state (around 6.0 × 10^{-6} mol photons in Fig. 5), before the polymer folds back into a conformation of the photostationary state. Measurements of the UV/Vis absorbance and calculation of the radius of gyration in MD underpin the initial intermittent unfolding, where the number of crosslinks is, for a short time, lower than in the photostationary state. The MD simulations offer an explanation for this effect: for individual conformers the dimerization ratio and radius of gyration fluctuate constantly, with the latter experiencing much greater variation, indicating a timescale difference between bond recombination and the morphology changes. Bond recombination is limited by the orientation and steric hindrance between styrylpyrene units. As the folded polymer is released from an almost completely locked conformation, the exploration of phase space regulated by the faster diffusion enables the polymer to explore configurations in a wider range beyond the equilibrium ensemble. In the thermodynamic limit, the photostationary state is retrieved by the slower process of bond recombination.

Fig. 5 a illustrates that simulations for **P1** show good agreement for dimerization ratios and radius of gyration in comparison with UV/vis and SEC measurements in all 3 experimental protocols: exclusive 430 nm, 330 nm irradiation, and dynamic unfolding of compact **SCNP1** from 430 nm irradiation followed by subsequent 330 nm irradiation. Simulation parameters obtained from fitting the **SCNP1** system were transferred to the longer **SCNP1′** (Fig. S12–S14†). We observe a comparable intermittent overshoot in the unfolding followed by a gradual return to its photostationary state, with results following the trend of the experiment. While in **P1** the shorter segmental lengths between crosslinked styrylpyrene results in more constrained conformer shapes,[40] in the longer **P1′** the diffusion constraints are less profound, which leads a weaker overshoot than for **P1**.

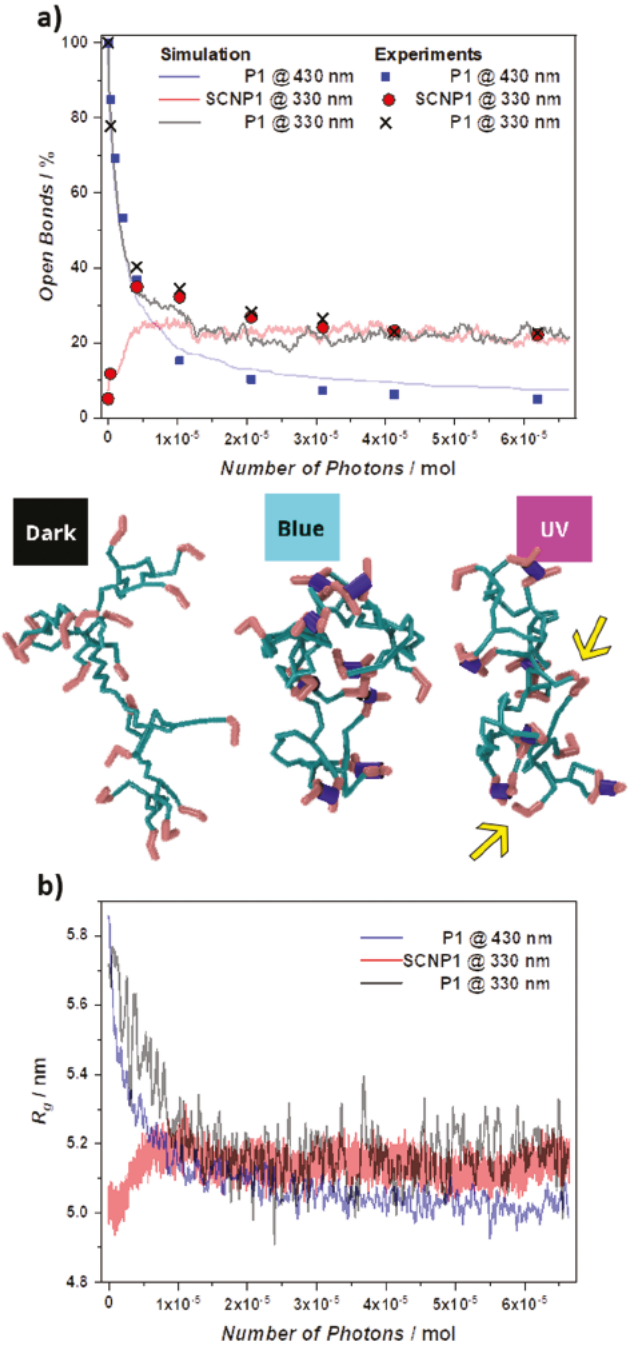

Fig. 5 (a) Comparison of experimentally determined number of open bonds and theoretically predicted number of open bonds from the MD simulation of P1 and SCNP1 under irradiation of different wavelengths, and snapshots of 3 distinct states during folding. The polymer chain P1 folds into a photostationary state, represented in the conformer snap shot "UV", either from the polymer coil (snapshot "Dark"), or from the compact SCNP1 (snapshot "Blue"). An intermittent overshoot in the unfolding of SCNP1@330nm (marked with red arrow) is observed due to the timescale separation between bond recombination and monomer diffusion. The conformer snapshot in the photostationary state is of a less compact conformation compared to SCNP1, the difference in crosslinks marked in yellow arrows. (b) Radius of gyration (R_g) as obtained from the MD simulation of P1 and SCNP1 under irradiation of different wavelengths.

Summary of experimental and theoretical findings

Combining the experimental and theoretical results, we observed that photocycloreversions of the stilbene derivative styrylpyrene are controlled by the confined environment of single polymer chains. Irradiation of styrylpyrene containing polymers with blue light (430 nm) triggers selectively intramacromolecular photocycloadditions, which induce single chain folding into an SCNP. However, subsequent irradiation with UV light (330 nm) induces a photostationary state, where photocycloreversion and photocycloaddition occur concomitantly. As a result, only a partial reversion of photocycloadducts was observed and a full unfolding of the SCNP into its linear parent polymer was not possible. Over the course of UV irradiation, the number of reverted photocycloadducts initially increases before it decreases again reaching a photostationary state, where the majority of bonds remained closed. Coarse-grained molecular dynamics simulations replicated the dynamic intermittent partial unfolding of the photostationary states induced by 430 nm or 330 nm light and elucidate the reasons for the intermittent overshoot in the unfolding of the SCNP. Irradiation of the linear parent polymer with blue light initiates exclusively the photocycloaddition reaction. As a consequence, once a covalent folding point is formed, it cannot be altered, even if over the course of the folding a different intramolecular architecture might become energetically more favourable. Once the irradiation wavelength is changed to UV light, both photocycloaddition and -reversion can occur concomitantly allowing a reshuffling of the bonds. The dynamic covalent nature of the SCNP under UV light was further supported by direct irradiation of the parent polymer with UV light, reaching both a comparable number of crosslinks and degree of compaction compared to the previously formed SCNPs.

Conclusions

The wavelength gated selectivity of photocycloaddition and -reversion that has been demonstrated for hydroxyl-styrylpyrene and polymers carrying terminal styrylpyrene moieties is lost in the strongly confined environment of single polymer chains, due to altered reaction kinetics. UV light Irradiation induces a photostationary state, where bond forming cycloaddition and bond cleaving cycloreversion occur concomitantly. In this state, bonds are constantly formed and broken, whereas the photocycloaddition remained the predominant reaction. As a consequence, covalent bonds can dynamically reshuffle within the crosslinked polymer chain, whereas an unfolding into the linear parent polymer is not possible. The herein investigated single polymer chains can be portrayed as small individual polymer networks. The observed strongly limited photocycloreversion in confined environments will translate into the more complex networks of polymer materials. We submit that addressing this critical photostationary state of photocycloadditions, that occurs within confined polymer matrices, is paramount to enable photocycload-

ditions as wavelength-gated, reversible binding sites in polymer materials. Ultimately we may be able to establish a purely light-gated control over crosslinked polymer networks, which has the potential to enable the recycling of polymer materials that are highly challenging to recycle conventionally such as thermosets.

Conflicts of interest

There are no conflicts to declare.

Acknowledgements

M. L. and W. W. acknowledge support from Deutsche Forschungsgemeinschaft (DFG, German Research Foundation) *via* the Collaborative Research Center "Molecular Structuring of Soft Matter" (SFB1176) and the Excellence Cluster "3D Matter Made to Order" (3DMM2O). H. F. acknowledges Prof. Christopher Barner-Kowollik (QUT) for sponsoring and mentorship of H. F.'s research activities in the context of his ARC Laureate Fellowship. The authors thank Dr Sarah Walden (QUT) for critical reading of the manuscript. H. F. acknowledges support by the Australian Research Council (ARC) in the form of a DECRA Fellowship as well as continued support from the Queensland University of Technology (QUT) through the Centre for Materials Science.

Notes and references

1 E. J. Foster, E. B. Berda and E. W. Meijer, *J. Am. Chem. Soc.*, 2009, **131**, 6964–6966.
2 T. Terashima, T. Mes, T. F. A. De Greef, M. A. J. Gillissen, P. Besenius, A. R. A. Palmans and E. W. Meijer, *J. Am. Chem. Soc.*, 2011, **133**, 4742–4745.
3 J. B. Beck, K. L. Killops, T. Kang, K. Sivanandan, A. Bayles, M. E. Mackay, K. L. Wooley and C. J. Hawker, *Macromolecules*, 2009, **42**, 5629–5635.
4 H. Rothfuss, N. D. Knöfel, P. W. Roesky and C. Barner-Kowollik, *J. Am. Chem. Soc.*, 2018, **140**, 5875–5881.
5 J. Rubio-Cervilla, E. González and J. A. Pomposo, *Nanomaterials*, 2017, **7**, 341.
6 J. Pomposo, *SINGLE-CHAIN POLYMER NANOPARTICLES: Synthesis, Characterization, Simulations, and Applications*, 2017.
7 S. Mavila, O. Eivgi, I. Berkovich and N. G. Lemcoff, *Chem. Rev.*, 2016, **116**, 878–961.
8 H. Frisch, B. T. Tuten and C. Barner-Kowollik, *Isr. J. Chem.*, 2020, **60**, 86–99.
9 J. Chen, J. Wang, Y. Bai, K. Li, E. S. Garcia, A. L. Ferguson and S. C. Zimmerman, *J. Am. Chem. Soc.*, 2018, **140**, 13695–13702.
10 J. Chen, J. Wang, K. Li, Y. Wang, M. Gruebele, A. L. Ferguson and S. C. Zimmerman, *J. Am. Chem. Soc.*, 2019, **141**, 9693–9700.
11 Y. Bai, X. Feng, H. Xing, Y. Xu, B. K. Kim, N. Baig, T. Zhou, A. A. Gewirth, Y. Lu, E. Oldfield and S. C. Zimmerman, *J. Am. Chem. Soc.*, 2016, **138**, 11077–11080.
12 R. Lambert, A.-L. Wirotius, S. Garmendia, P. Berto, J. Vignolle and D. Taton, *Polym. Chem.*, 2018, **9**, 3199–3204.
13 Y. Liu, S. Pujals, P. J. M. Stals, T. Paulöhrl, S. I. Presolski, E. W. Meijer, L. Albertazzi and A. R. A. Palmans, *J. Am. Chem. Soc.*, 2018, **140**, 3423–3433.
14 E. Huerta, P. J. M. Stals, E. W. Meijer and A. R. A. Palmans, *Angew. Chem., Int. Ed*, 2013, **52**, 2906–2910.
15 N. D. Knöfel, H. Rothfuss, J. Willenbacher, C. Barner-Kowollik and P. W. Roesky, *Angew. Chem., Int. Ed*, 2017, **56**, 4950–4954.
16 Y. Liu, P. Turunen, B. F. M. de Waal, K. G. Blank, A. E. Rowan, A. R. A. Palmans and E. W. Meijer, *Mol. Syst. Des. Eng.*, 2018, **3**, 609–618.
17 R. Lambert, A.-L. Wirotius, J. Vignolle and D. Taton, *Polym. Chem.*, 2019, **10**, 460–466.
18 T. S. Fischer, D. Schulze-Sünninghausen, B. Luy, O. Altintas and C. Barner-Kowollik, *Angew. Chem., Int. Ed.*, 2016, **55**, 11276–11280.
19 J. Willenbacher, B. V. K. J. Schmidt, D. Schulze-Suenninghausen, O. Altintas, B. Luy, G. Delaittre and C. Barner-Kowollik, *Chem. Commun.*, 2014, **50**, 7056–7059.
20 T. S. Fischer, S. Spann, Q. An, B. Luy, M. Tsotsalas, J. P. Blinco, H. Mutlu and C. Barner-Kowollik, *Chem. Sci.*, 2018, **9**, 4696–4702.
21 B. Tuten, D. Chao, C. Lyon and E. B. Berda, *Polym. Chem.*, 2012, **3**, 3068–3071.
22 A. Levy, R. Feinstein and C. E. Diesendruck, *J. Am. Chem. Soc.*, 2019, **141**, 7256–7260.
23 N. Hosono, A. M. Kushner, J. Chung, A. R. A. Palmans, Z. Guan and E. W. Meijer, *J. Am. Chem. Soc.*, 2015, **137**, 6880–6888.
24 H. Frisch, J. P. Menzel, F. R. Bloesser, D. E. Marschner, K. Mundsinger and C. Barner-Kowollik, *J. Am. Chem. Soc.*, 2018, **140**, 9551–9557.
25 Y. Liu, T. Pauloehrl, S. I. Presolski, L. Albertazzi, A. R. A. Palmans and E. W. Meijer, *J. Am. Chem. Soc.*, 2015, **137**, 13096–13105.
26 T. Mes, R. van der Weegen, A. R. A. Palmans and E. W. Meijer, *Angew. Chem., Int. Ed.*, 2011, **50**, 5085–5089.
27 H. Frisch, F. R. Bloesser and C. Barner-Kowollik, *Angew. Chem., Int. Ed.*, 2019, **58**, 3604–3609.
28 J. T. Offenloch, E. Blasco, S. Bastian, C. Barner-Kowollik and H. Mutlu, *Polym. Chem.*, 2019, **10**, 4513–4518.
29 E. Verde-Sesto, A. Blázquez-Martín and J. A. Pomposo, *Polymers*, 2019, **11**, 1903.
30 H. Frisch, D. E. Marschner, A. S. Goldmann and C. Barner-Kowollik, *Angew. Chem., Int. Ed*, 2017, **57**, 2036–2045.
31 J. He, L. Tremblay, S. Lacelle and Y. Zhao, *Soft Matter*, 2011, **7**, 2380–2386.
32 P. G. Frank, B. T. Tuten, A. Prasher, D. Chao and E. B. Berda, *Macromol. Rapid Commun.*, 2014, **35**, 249–253.
33 T. Doi, H. Kawai, K. Murayama, H. Kashida and H. Asanuma, *Chem. – Eur. J.*, 2016, **22**, 10533–10538.

34 V. X. Truong, F. Li, F. Ercole and J. S. Forsythe, *ACS Macro Lett.*, 2018, 7, 464–469.
35 D. E. Marschner, H. Frisch, J. T. Offenloch, B. T. Tuten, C. R. Becer, A. Walther, A. S. Goldmann, P. Tzvetkova and C. Barner-Kowollik, *Macromolecules*, 2018, **51**, 3802–3807.
36 H. Frisch, K. Mundsinger, B. L. J. Poad, S. J. Blanksby and C. Barner-Kowollik, *Chem. Sci.*, 2020, **11**, 2834–2842.
37 N. P. Kovalenko, A. Abdukadirov, V. I. Gerko and M. V. Alfimov, *J. Appl. Spectrosc.*, 1980, **32**, 607–612.
38 P. J. Hoogerbrugge and J. M. V. A. Koelman, *EPL Europhys. Lett.*, 1992, **19**, 155.
39 R. D. Groot and P. B. Warren, *J. Chem. Phys.*, 1997, **107**, 4423–4435.
40 D. Danilov, C. Barner-Kowollik and W. Wenzel, *Chem. Commun.*, 2015, **51**, 6002–6005.